Histol Histopathol (2021) 36: 853-867

http://www.hh.um.es

Histology and Histopathology
From Cell Biology to Tissue Engineering

ORIGINAL ARTICLE **Open Access**

Maternal protein restriction changes structural and metabolic gene expression in the skeletal muscle of aging offspring rats

Jéssica Silvino Valente[1], Érika Stefani Perez[1], Bruna Tereza Thomazini Zanella[1], Tassiana Gutierrez de Paula[1], Sérgio Alexandre Alcantara dos Santos[1], Bruno Oliveira da Silva Duran[2], Robson Francisco Carvalho[1], Luis Antonio Justulin[1], Bruno Evaristo de Almeida Fantinatti[1,3] and Maeli Dal-Pai-Silva[1]

[1]Department of Structural and Functional Biology, Institute of Biosciences, São Paulo State University (UNESP), Botucatu, São Paulo, [2]Department of Histology, Embryology and Cell Biology, Institute of Biological Sciences, Federal University of Goiás (UFG), Goiânia, Goiás and [3]University Ninth of July (UNINOVE), Bauru, São Paulo, Brazil

Summary. Maternal protein restriction affects postnatal skeletal muscle physiology with impacts that last through senility. To investigate the morphological and molecular characteristics of skeletal muscle in aging rats subjected to maternal protein restriction, we used aged male rats (540 days old) born of dams fed a protein restricted diet (6% protein) during pregnancy and lactation. Using morphological, immunohistochemical and molecular analyses, we evaluated the soleus (SOL) and extensor digitorum longus (EDL) muscles, muscle fiber cross-sectional area (CSA) (n=8), muscle fiber frequency (n=5) and the gene expression (n=8) of the oxidative markers (succinate dehydrogenase-*Sdha* and citrate synthase-*CS*) and the glycolytic marker (lactate dehydrogenase-*Ldha*). Global transcriptome analysis (n=3) was also performed to identify differentially regulated genes, followed by gene expression validation (n=8). The oxidative SOL muscle displayed a decrease in muscle fiber CSA (*p<0.05) and in the expression of oxidative metabolism marker *Sdha* (***p<0.001), upregulation of the anabolic *Igf-1* (**p<0.01), structural Chad (**p<0.01), and *Fmod* (*p<0.05) genes, and downregulation of the *Hspb7* (**p<0.01) gene. The glycolytic EDL muscle exhibited decreased IIA (*p<0.05) and increased IIB (*p<0.05) fiber frequency, and no changes in muscle fiber CSA or in the expression of oxidative metabolism genes. In contrast, the gene expression of *Chad* (**p<0.01) was upregulated and the *Myog* (**p<0.01) gene was downregulated. Collectively, our morphological, immunohistochemical and molecular analyses showed that maternal protein restriction induced changes in the expression of metabolic, anabolic, myogenic, and structural genes, mainly in the oxidative SOL muscle, in aged offspring rats.

Key words: Skeletal muscle, Maternal protein restriction, Gene expression

Corresponding Author: Maeli Dal-Pai-Silva, PhD, Rua Prof. Dr. Antônio Celso Wagner Zanin, 250, Distrito de Rubião Junior, Botucatu, SP - 18618-689, Brazil. e-mail: maeli.dal-pai@unesp.br

DOI: 10.14670/HH-18-337

Introduction

Inadequate maternal nutrition during pregnancy and/or lactation promotes changes in fetal genotype and development, impairing postnatal physiology, a condition named fetal programming (Barker, 1998, 2004; Hales and Barker, 2001). This concept gives rise to the "developmental origins of health and disease" (DOHaD), which links the early life exposure to adverse conditions to the increased incidence of disease with age (Hanson, 2015). Fetal programming is associated with epigenetic alterations that modulate gene expression and may help to explain the changes in skeletal muscle phenotype in offspring exposed to maternal undernutrition (Cabeço et al., 2012; Confortim et al., 2017; Kalbe et al., 2017).

The phenotypic diversity of skeletal muscles is a contributing factor to the distinct responses to experimentally induced stimulation, such as physical exercise (Leandro et al., 2012; Vechetti-Júnior et al., 2013), immobilization (Carlson et al., 2009; Vechetti et al., 2016), aging (Caccia et al., 1979; Domingues-Faria et al., 2016), and maternal protein restriction (Cabeço et al., 2012; Confortim et al., 2017). In addition to muscle diversity, the use of different animal models can also

contribute to variations in the responses found in studies that assessed the effects of maternal nutrient restriction on offspring skeletal muscle throughout life (Mallinson et al., 2007; Raja et al., 2016; Kalbe et al., 2017). In murine models, maternal protein restriction promoted a decrease in the body weight of offspring accompanied by molecular and morphological changes in muscle fiber area, number and frequency, and in the gene expression of the myogenic regulatory factors (MRFs) (Toscano et al., 2008; Cabeço et al., 2012; Confortim et al., 2017). Maternal protein restriction also alters the skeletal muscle phenotype and neuromuscular junctions in aging (Confortim et al., 2015). Beyond these changes in muscle fibers, some components of the extracellular matrix (ECM), such as collagen, can also be affected in aging (Confortim et al., 2015).

The ECM, together with blood and nervous tissue, constitutes the muscle microenvironment indispensable for the maintenance of the functional and morphological integrity of skeletal muscle fibers (Voytik et al., 1993; Velleman, 1999; Theocharis et al., 2016; Stearns-Reider et al., 2017). The ECM is an amalgam of cells and molecules, such as collagen, fibronectin, laminin, and proteoglycans, which provides mechanical support and has close chemical and functional communication with skeletal muscle (Mendias et al., 2017; Stearns-Reider et al., 2017; Ahmad et al., 2018). To better understand skeletal muscle remodeling during intrauterine and postnatal development in response to maternal protein restriction, it is essential to consider the structure and functions of the muscle microenvironment (muscle fibers and the ECM) in this condition (Talbert and Guttridge, 2016; Mendias et al., 2017; Ahmad et al., 2018).

In this study, we evaluated structural and metabolic gene expression in the skeletal muscle of aged rats, born from dams fed a protein restricted diet during pregnancy and lactation. We hypothesized that maternal perinatal protein restriction changes the gene expression of components of the muscle microenvironment, including muscle fibers and the ECM, in aging offspring rats.

Table 1. Diet ingredients used in the experiment.

Ingredients	Standard diet (17% protein) g/kg	Hypoproteic diet (6%protein) g/kg
Casein (84% protein)	202	71.5
Starch	397	480
Dextrin	130.5	159
Sucrose	100	121
L-cystine	3	1
Fiber pH 101 or pH 102 (microcellulose)	50	50
Soy oil	70	70
Mixture of salts AIN93G**	35	35
Mixtura of vitamins AIN93G**	10	10
Choline Hydrochloride or Choline Bitartrate	2.5	2.5

** to know the detailed composition of the mix of salts and vitamins, consult Reeves et al., 1993. The Diet is elaborated by the company PragSoluções (PragSoluções, Jaú, SP, Brazil).

Materials and methods

Ethics statement

The experiments were conducted according to the Arrive Guideline (Kilkenny et al., 2010), following the Ethical Principles of Animal Experimentation adopted by the Brazilian College of Animal Experimentation (COBEA) and approved by the Animal Experimentation Ethics Committee of UNESP (Protocol number 573). Only males were used to avoiding the interference of the hormonal oscillations of the females in the experiment. Every effort has been made to minimize animal suffering. They were anesthetized intraperitoneally with the combined use of general anesthetic followed by rodent guillotine euthanasia.

Samples collection

Sprague Dawley male rats (n=4) and female (n=8), in reproductive age (90 days old), were supplied by the Bioethics Center of the State University of Campinas (Campinas, SP, Brazil). The animals housed in polypropylene cages were kept under controlled conditions of temperature (22°C to 25°C), relative humidity (55%), and photoperiod (12h) with food and water *ad libitum*. After mating of virgin females with breeding males and detection of sperm through vaginal smear, pregnant females were divided into two experimental groups: Control females (n=4): fed a standard diet (17% protein) and Restricted females (n=4): fed a hypoproteic diet (6% protein), during pregnancy and lactation. The standard diet (17% protein) was provided by Institute of Biosciences, Botucatu/UNESP and the hypoproteic diet (6% protein) was obtained from PragSoluções (PragSoluções, SP, Brazil) (Table 1). All diets have been used in previous studies (Cabeço et al., 2012; Santos et al., 2018). To maximize lactation, after birth, offspring were reduced to eight pups (1:1 ratio between males and females). After weaning, only the males were used in the experiments. Animals were kept in the box, under the light and temperature conditions mentioned above, with standard diet and water *ad libitum*. The offspring were composed of two groups, according to maternal feeding during pregnancy and lactation: Control Group (CG) (n=16): pups from dams fed a standard diet and Restricted Group (RG) (n=16): pups from dams fed a hypoproteic diet. Due to the high mortality rates at aging (540 days), a high number of offspring (n=16) was initially used, considering that most of the experiments were conducted with 8 offspring males per group. At the end of the experiment (540 days old), the animals were weighed, anesthetized, and euthanized. Samples of the soleus (SOL) and extensor digital longus (EDL) muscles were collected, frozen in liquid nitrogen, and submitted to morphological, immunohistochemical, and molecular

analyses. Epididymal, retroperitoneal and visceral fats were also collected and weighed, which together were considered as total body fat.

Morphological data

Histological sections from SOL and EDL muscles (10 μm), obtained in a cryostat Leica (CM1850 – Leica Biosystems) at -20°C, were submitted to hematoxylin-eosin (H&E) (n=8) and picrosirius red staining (n=5) to evaluate the muscle morphology and cross-sectional area (CSA), and collagen percentage quantification, respectively. Random images were obtained (~4 histological fields, 20x magnification) using a compound microscope attached to a computerized imaging analysis system (Leica Qwin, Wetzlar, Germany). Approximately, the CSA of 400 muscle fibers were measured using Image Analysis System Software (Image J 1.50i) (Schneider et al., 2012) and distributed in the following classes (≤1000, 1001≤2000, 2001≤3000, 3001≤4000, 4001≤5000, ≥5001 μm). Muscle fiber area distribution in class corresponded to the number of fibers from each area class relative to the total number of fibers measured. The collagen percentage and the collagen fractal dimension were assessed in two random fields of each muscle/animal, using Image Analysis System Software (Leica Qwin, Germany), following the software instructions for collagen quantification. The collagen fractal dimension was measured using Image Analysis System Software (Image J 1.50i) (Schneider et al., 2012).

Immunohistochemical reaction

Histological tissue sections (7 μm) from SOL and EDL muscles were obtained in a cryostat (JUNG CM1800, Leica Germany) at -20°C. Samples (n=5) were initially hydrated with PBS and incubated with the specific primary antibodies (Myosin Type I: BA. D5 IgG2b; Type IIA: SC.71 IgG1; Type IIB: BF. F3 IgM (Developmental Studies Hybridoma Bank: http://dshb.biology.uiowa.edu/)) for 90 minutes at room temperature (Table 2). Next, the samples were incubated with appropriate fluorescent - conjugated secondary antibodies: (Goat anti-ms IgG2b, Alexa Fluor 647 (Cy5-pink) conjugated 2 nd AB (Invitrogen, A21242); Goat anti-ms IgG1, Alexa Fluor 488 (green) conjugated 2 nd AB (Invitrogen, A21121); Goat anti-ms IgM, Alexa Fluor 555 (red) conjugated 2nd AB (Invitrogen, A-21426) (Table 2), for 60 minutes at room temperature. Subsequently, samples were washed with PBS, fixed in methanol, and mounted with Fluorescent Vectashield (H-1000 - Vector Laboratories). We used imilar immunohistochemical protocol described by Wen et al. (2018). Muscle fiber type frequency was analyzed using four histologial fields per animal (20x Lens, ~400). The images were captured by Confocal Microscope TCS SP5 (Leica Microsystems, UK) and analyzed using Image Analysis Software (Image J 1.50i) (Schneider et al., 2012).

Table 2. Specification for antibodies used in immunofluorescence reaction.

Name	Catalog number	Dilution	Company
Primary			
IgG2b	BA-D5	1:100	Hybridoma Bank
IgG1	SC-71	1:100	Hybridoma Bank
IgM	BF-F3	1:100	Hybridoma Bank
Secondary			
Goat anti-ms IgG2b Alexa Fluor 647	A-21242	1:250	Invitrogen
Goat anti-ms IgG1 Alexa Fluor 488	A-21121	1:500	Invitrogen
Goat anti-ms IgM Alexa Fluor 555	A-21426	1:250	Invitrogen

RNA extraction and sequencing libraries

Samples of SOL and EDL muscles were frozen in liquid nitrogen (n=3) and total RNA was extracted using the TRIzol protocol, following the manufacturer's specifications. The purified RNA was resuspended in Ultrapure Water and stored at -80°C. The quality of RNA extraction and quantification were verified using the Nano Vue Plus spectrophotometer (GE HealthCare, USA), and RNA Integrity Number (RIN) was obtained through the analysis of microfluidic ribosomal RNAs using the 2100 Bioanalyzer system (Agilent, USA) (Fleige and Pfaffl, 2006). We used only samples with RIN equal or higher than 8,0. The entire library generation and mRNA sequencing were performed by LC Sciences, Houston TX (USA), and the transcriptome was obtained by Illumina HiSeq 2500 Fast Mode (Illumina, USA).

Bioinformatics Analyses

The analyses of the data obtained through the sequencing was performed based on a high-performance computational structure located in the Laboratory of Biology of Striated Muscle (LBME). It consists of a data-processing station based on a total of 64 gigabytes of memory and 24threads. In terms of software, the data were given through the GNU/Linux operating system, based on the Linux Mint distribution 18.3 (available at http://www.linuxmint.com).

The data were first analyzed for the read quality of the sequencing using FastQC software (http://www.bioinformatics.babraham.ac.uk/projects/fastqc) version 0.10.1. After the analysis of quality, the data went through a process of quality filtering and removal of adapters using Trimmomatic software (Bolger et al., 2014). The libraries were then aligned against the *Rattus novergicus* genome (version 6.0) by using Hisat2 software (Li and Dewey, 2011; Yang and Kim, 2015). The software featureCounts (Liao et al., 2014) was used to extract the read numbers for each annotated gene, allowing expression analysis using the R / Bioconductor DESeq2 (Anders and Huber, 2010). The genes were considered differentially expressed when log2 Fold

Change ≥1 for upregulated genes and log2 Fold Change ≤1 for downregulated genes, and adjusted p-value set ≤0.05.

Gene expression analysis of mRNAs by RT-qPCR

The RT-qPCR procedures followed the guidelines of the MIQE: Minimum Information for Publication of Quantitative Real-Time PCR Experiment.

After the extraction of the total RNA from the muscle samples (n=8), its quality was obtained by RNA Integrity Number (RIN), from the analysis of the ribosomal RNAs based on microfluidics, using the 2100 Bioanalyzer system (Agilent, USA) (Fleige and Pfaffl, 2006). Only samples with RIN equal to or higher than 8,0 were used. The cDNA was obtained by reverse transcription (RT) reaction using the High Capacity cDNA Archive kit (Life Technologies Corporation, Carlsbad, CA, USA), according to the manufacturer's specification. The cDNA samples were amplified using the Power SYBR Green Mix (2.5x) - Promega. The mRNA expression levels were measured by RT-qPCR through the Quant Studio System (Applied Biosystems, Foster City, CA, USA), and the reactions for each gene were performed in duplicate. The thermocycling conditions of the RTq-PCR reaction were standardized according to the instructions of the equipment manufacturer. Metabolic and myogenic genes as well as genes selected by the transcriptome were validated using an endogenous gene, *Ppia* (Tables 3, 4). Relative quantification of gene expression was performed using the comparative CT method (Livak and Schmittgen, 2001) using DataAssist 2.0 (Life Technologies).

Table 3. Genes analyzed in the RT-qPCR with primers sequence drawn from the GenBank.

Primer	Primer Sequence
Myod F	5' CCAAATGGACTGGTCCCGAA 3'
Myod R	5' AGCCCACGAAGAGTGTAATGA 3'
Myog F	5' CCCAGTGAATGCAACTCCCA 3'
Myog R	5' CGAGCAAATGATCTCCTGGGT 3'
Igf-1 F	5´TTCAGTTCGTGTGTGGACA 3'
Igf-1 R	5' TCCGAATGCTGGAGCCATAG 3'
Mafbx F	5' GACCTGCATGTGCTCAGTGAAG 3'
Mafbx R	5' GGATCTGCCGCTCTGAGAAGT 3'
Murf1 F	5´TGGAGATGCAATTGCTCAGT 3'
Murf1 R	5' GTGAAGTTGCCCCCTTACAA 3'
Sdha F	5' TCCTTCCCACTGTGCATTACAA 3'
Sdha R	5' CGTACAGACCAGGCACAATCTG 3'
CS F	5' CATGACGGTGGCAATGTAAG 3'
CS R	5' CCATTCATAGCTGCTGCAAA 3'
Ldha F	5' CCGTTACCTGATGGGAGAAA 3'
Ldha R	5' ACGTTATTCACACCACTCCACAC 3'
Ppia* F	5' TCAACCCCACCGTGTTCTTC 3'
Ppia* R	5' ACTTTGTCTGCAAACAGCTCG 3'

*Endogenous gene.

Statistical Analyses

All statistical analyses were performed using GraphPad Prism version6.01. For the results with normal distribution, we used the Unpaired Student's T test to compare the experimental groups. For the data that did not get the normal distribution, the Unpaired Mann Whitney test was used. The significance level considered was 5% ($p<0.05$). Data are expressed as mean ± SEM.

Results

Anatomic data

The maternal protein restriction diet decreased body weight (***$p<0.001$), and total body fat (*$p<0.05$) of the offspring from the restricted group (RG) compared to the control group (CG), at 540 days old (Fig. 1).

Morphological and Immunohistochemical data

Both muscles showed normal morphology, with polygonal and round shape muscle fibers and peripheral nuclei. Muscle fibers were organized in fascicles by connective tissue, the perimysium, and each muscle fiber was surrounded individually by a thin layer of connective tissue, the endomysium (Figs. 2a, 3a). Muscle fiber cross-section area (CSA) decreased only in the SOL muscle of the RG compared to the CG animals, with a decrease in the muscle fiber class with a larger area (3001-5000 μm) and increase in muscle fiber class with a lower area (1001-2000 μm) (*$p<0.05$) (Figs. 2b, 3b). There were no changes in collagen distribution in the SOL and EDL muscles (data no shown). There were no changes in the frequency of the muscle fiber types (I and IIA) in the SOL, whereas in the EDL muscle, the GR animals presented a decrease in the frequency of the type IIA (*$p<0.05$) and an increase in the frequency of

Table 4. Genes analyzed in the RT-qPCR with primers sequence obtained from the the genome of Rattus norvergicus.

Primer	Primer Sequence
Aqp7 F	5' GTTTGCGTTCTTGGGGTGTC 3'
Aqp7 R	5' ACGGGATGGGTTGATTGCAT 3'
Chad F	5' TTCCGCTGGAGAGACTACTGA 3'
Chad R	5' CGGGGTGGCTATAGGGAGT 3'
Fmod F	5' TGGATGGGAACGAGATCAAGC 3'
Fmod R	5' CAAGGCGAAGCCCCTCAGAT 3'
Hspb7 F	5' TCGCCATGACCCCTGACAAT 3'
Hspb7 R	5' GGGCCTAAGAGTGTGTGGAG 3'
Klf10 F	5' CAGCAAGGGTTACTCCCCAG 3'
Klf10 R	5' CACATCCTGGGTGGCTACAG 3'
c-Myc F	5' AGCCACCTAACTTTTCACCCT 3'
c-Myc R	5' GCTGTCAAGAATGAGTGTGCC 3'
Noct F	5' TCCGAGTGTGTGCTGTCATC 3'
Noct R	5' GCTACTCATGCCCCTAACGG 3'

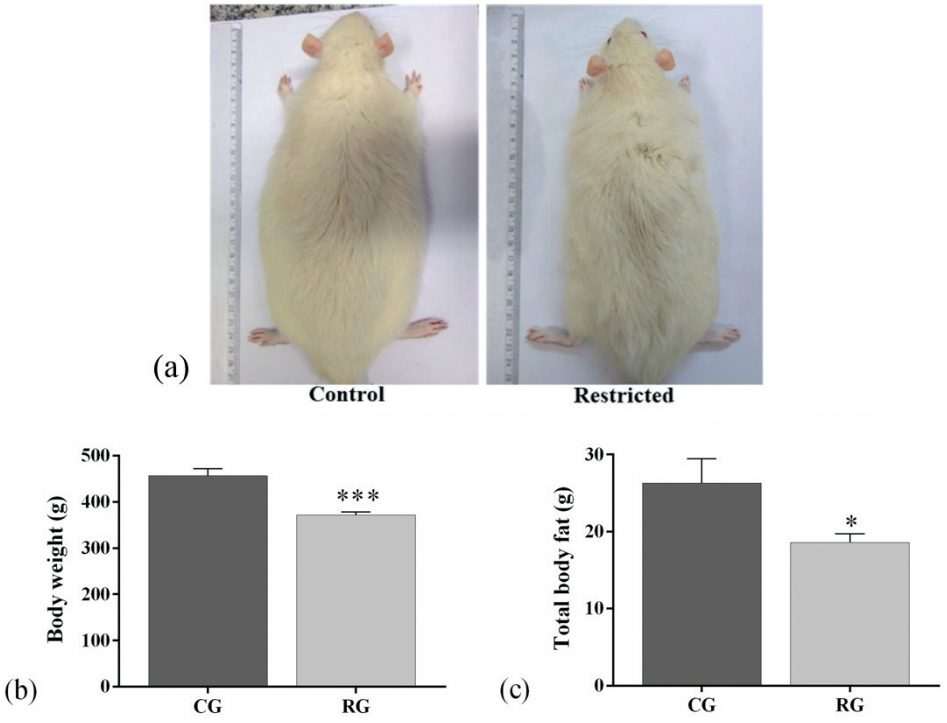

Fig. 1. Anatomic data in control group (CG) and restricted group (RG). Image of animals from control group (CG) and restricted group (RG), at 540 days old **(a)**. Body weight (g) **(b)** and total body fat (g) **(c)**, of CG and RG. The data are presented as the mean ± SEM (n=8). Unpaired Student's t-test. *p<0.05, ***p<0.001.

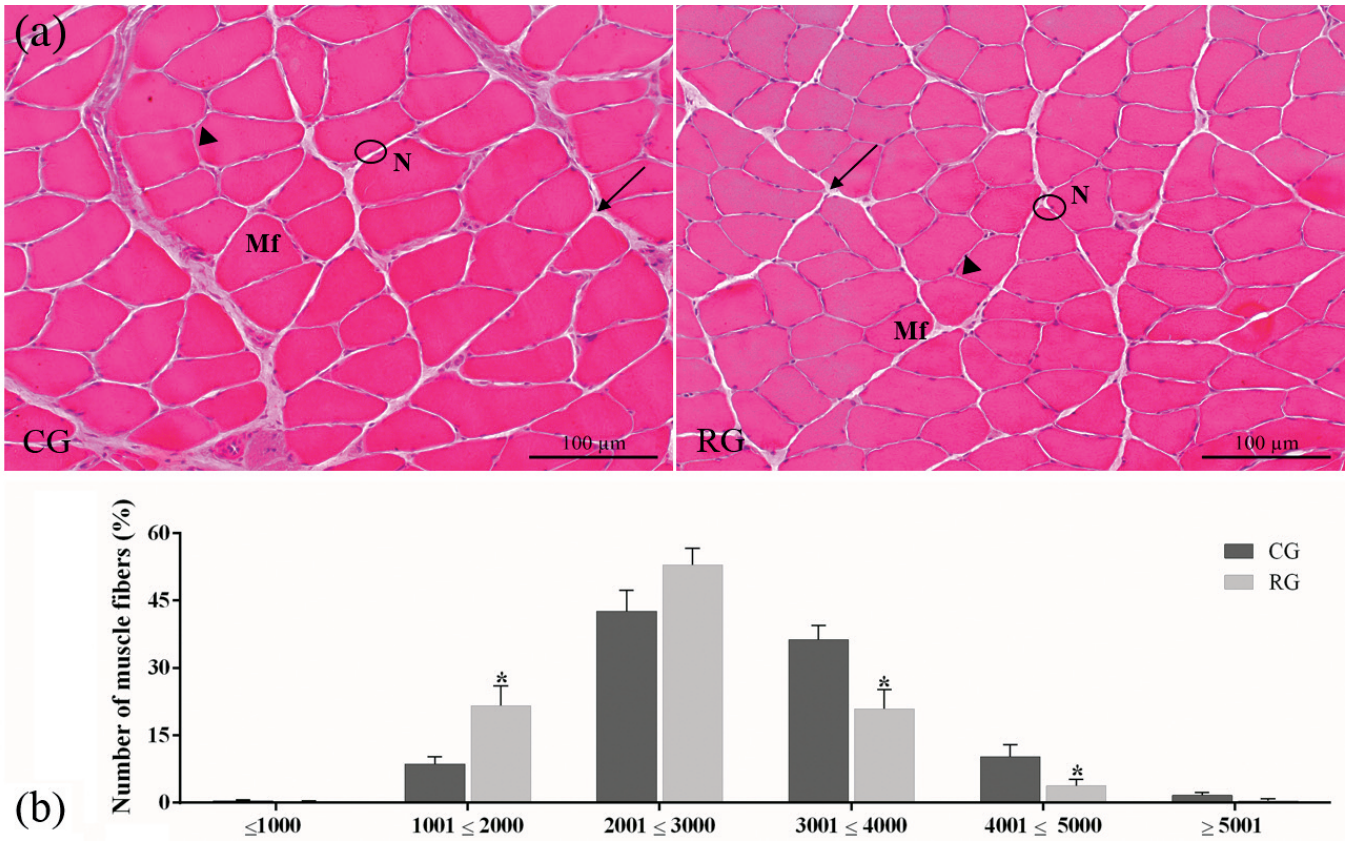

Fig. 2. SOL muscle fiber cross-sectional area from CG and RG groups. Histological section (10μm) highlighting the muscle fibers (Mf); perimysium (arrow); endomysium (arrowhead); peripheral nuclei (N) **(a)**. Graph showing an increase in the muscle fiber class with a lower area (1001-2000 μm) and decrease in muscle fiber class with a larger area (3001-5000 μm) **(b)**. The data are presented as the mean ± SEM (n=8). Unpaired Student's t-test. *p<0.05. Scale bars: 100 µm.

the type IIB fibers (*p<0.05), compared to the CG (Fig. 4, Table 5).

Expression of metabolic and myogenic genes by RT-qPCR

We evaluated the expression of genes involved with muscle oxidative (*Sdha* and *CS*) and glycolytic (*Ldha*) metabolism, catabolism (*Murf1* and *Mafbx*) and anabolism (*Igf-1*), and genes related with myogenic control (*Myod* and *Myog*). Only the SOL muscle

Table 5. Muscle fiber types frequency (%) in SOL and EDL muscles of the CG and RG groups.

	Type I	Type IIA	Type IIX	Type IIB
SOL				
CG	85.36±2.45%	14.64±2.45%		
RG	84.42±1.82%	15.58±1.82%		
EDL				
CG	3.39±1.15%	47.02±2.12%	24.27±4.79%	25.32±3%
RG	6.35±1.31%	30.43±9.15%*	20.4±3.06%	42.83±5.15%*

The data are presented as the mean and SEM (n=5). Unpaired Mann Whitney test. *p<0.05.

Table 6. Table showing read number throughout filtering process and total percentage of remaining reads after processing.

Samples	Raw	Paired	Orphaned	Paired (%)	Orphaned (%)
8_R1	26628791	18084786	7620373	67.9	28.6
8_R2	26628791	18084786	756914	67.9	2.8
9_R1	38235476	28385004	8630881	74.2	22.6
9_R2	38235476	28385004	1023106	74.2	2.7
12_R1	30115384	19877165	8743007	66.0	29.0
12_R2	30115384	19877165	1238938	66.0	4.1
13_R1	27606286	18392884	7506684	66.6	27.2
13_R2	27606286	18392884	1408205	66.6	5.1
15_R1	25314743	17264877	6589330	68.2	26.0
15_R2	25314743	17264877	1212012	68.2	4.8
28_R1	28386580	20607794	6449821	72.6	22.7
28_R2	28386580	20607794	1116467	72.6	3.9
29_R1	33594861	25397931	7149314	75.6	21.3
29_R2	33594861	25397931	866733	75.6	2.6
32_R1	30735116	21996090	6984394	71.6	22.7
32_R2	30735116	21996090	1459365	71.6	4.7
33_R1	30352825	22458874	6451386	74.0	21.3
33_R2	30352825	22458874	1233191	74.0	4.1
35_R1	32932860	24506432	6499534	74.4	19.7
35_R2	32932860	24506432	1665063	74.4	5.1
			Total Average	71.1	14.1

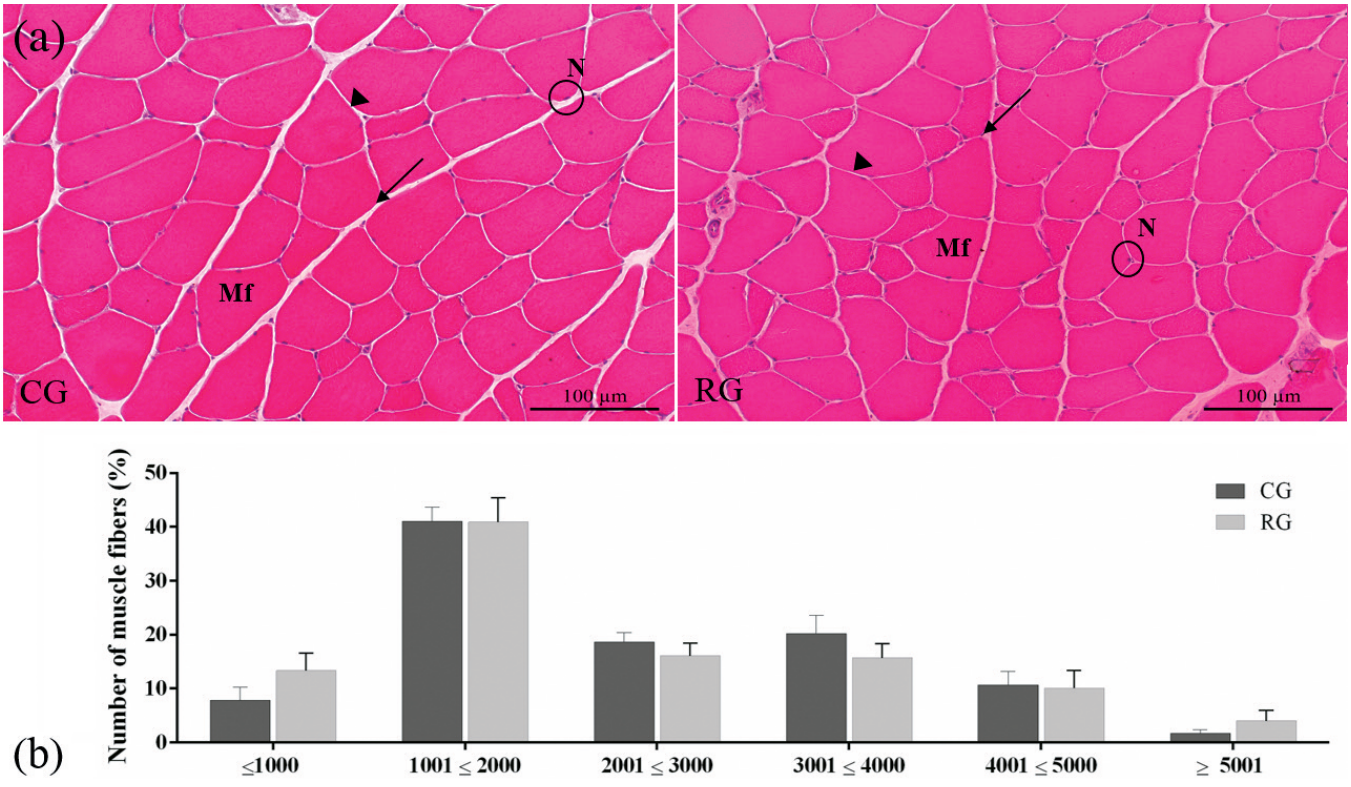

Fig. 3. EDL muscle fiber cross-sectional area from CG and RG groups. Histological section (10 μm) highlighting muscle fibers (Mf); perimysium (arrow); endomysium (arrowhead); peripheral nuclei (N) **(a)**. Graph showing no difference in EDL muscle area distribution in class **(b)**. The data are presented as the mean ± SEM (n=8). Unpaired Student's t-test. Scale bars: 100 µm.

presented a decreased gene expression of *Sdha* (***p<0.001) (Fig. 5), and increased gene expression of *Igf-1* (**p<0.01) in RG animals (Fig. 6a). The EDL muscle showed a decreased gene expression of *Myog* (**p<0.01) in RG compared to the CG animals (Fig. 6b). Gene expression of *Murf1, Mafbx,* and *Myod* did not change between the groups (Fig. 6).

Transcriptional profile and gene expression analyses by RT-qPCR

After alignment, read-count values were extracted. Expressed genes were obtained by removing all genes in which the sum of all samples is equal to zero counts. Out of 24219 genes annotated in the genome, 18242 genes were considered expressed in the libraries (Table 6).

Principal Component Analysis (PCA) showed a variation of 88% (PC1 + PC2) among the samples of CG and RG (Fig. 7a). As one CG sample for both SOL and EDL muscles clustered with the RG samples, we removed for further analyses. Then, the PCA without this sample was 89%. (Fig. 7b).

The differential expression genes (DEGs) analysis between CG and RG in the SOL muscle revealed 101 differentially regulated genes exclusively in RG (adj. p-value ≤0.05 and log2 Fold Change ≥1 and ≤1), of which 46 and 45 were upregulated and downregulated, respectively (Table 7). The EDL muscle revealed 53 differentially regulated genes exclusively in RG (adj. p-value ≤0.05 and log2 Fold Change ≥1 and ≤1), of which

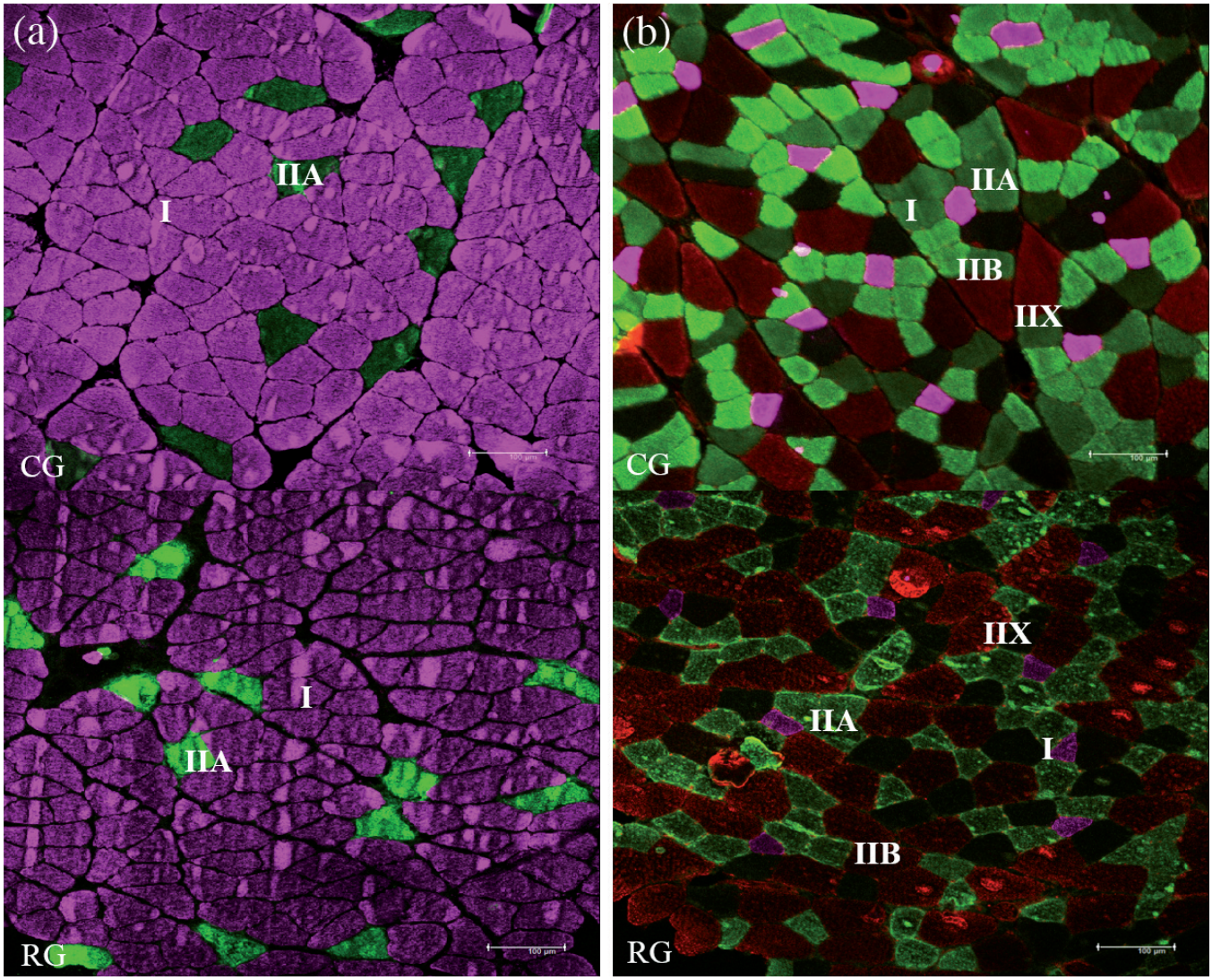

Fig. 4. Histological section (7 μm) of the immunohistochemical reaction of the SOL and EDL muscles from CG and RG groups. In the SOL muscle, showing muscle fibers type I (pink) and type IIA (green) **(a)**. In the EDL muscle, showing muscle fibers type I (pink), type IIA (green), type IIX (black) and type IIB (red) **(b)**. Scale bars: 100 μm.

20 and 30 were upregulated and downregulated, respectively (Table 8). As a parameter for choosing genes to validate for RT-qPCR, we selected seven common upregulated and downregulated DEGs in the SOL and EDL muscles. The genes upregulated (*Fmod* and *Chad*) and downregulated (*Noct, c-Myc, Klf10, Aqp7, Hspb7*) were validated using RT-qPCR. These genes are associated with muscle microenvironment (muscle fiber and ECM), biogenesis, structural function, and metabolism (Table 9).

The SOL muscle showed an increase in the expression of *Chad* gene (** p<0.01) and *Fmod* gene (*p<0.05) and decreased levels of *Hspb7* gene (**p<0.01) in RG compared to the CG group (Fig. 8a).

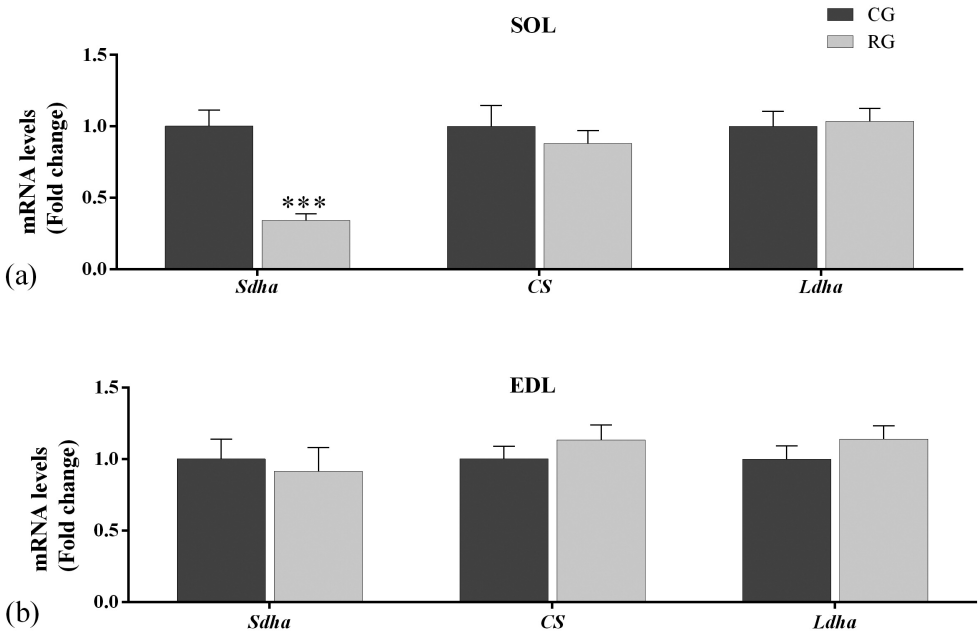

Fig. 5. Relative mRNA expression of oxidative and glycolytic metabolism genes in the SOL and EDL muscles of the CG and RG groups. mRNA levels of the Sdha, CS and Ldha of the SOL muscle **(a)**. mRNA levels of the Sdha, CS and Ldha of the EDL muscle **(b)**. The data are expressed as fold change and are presented as the mean ± SEM (n=8). Unpaired Mann Whitney test. ***p<0.001.

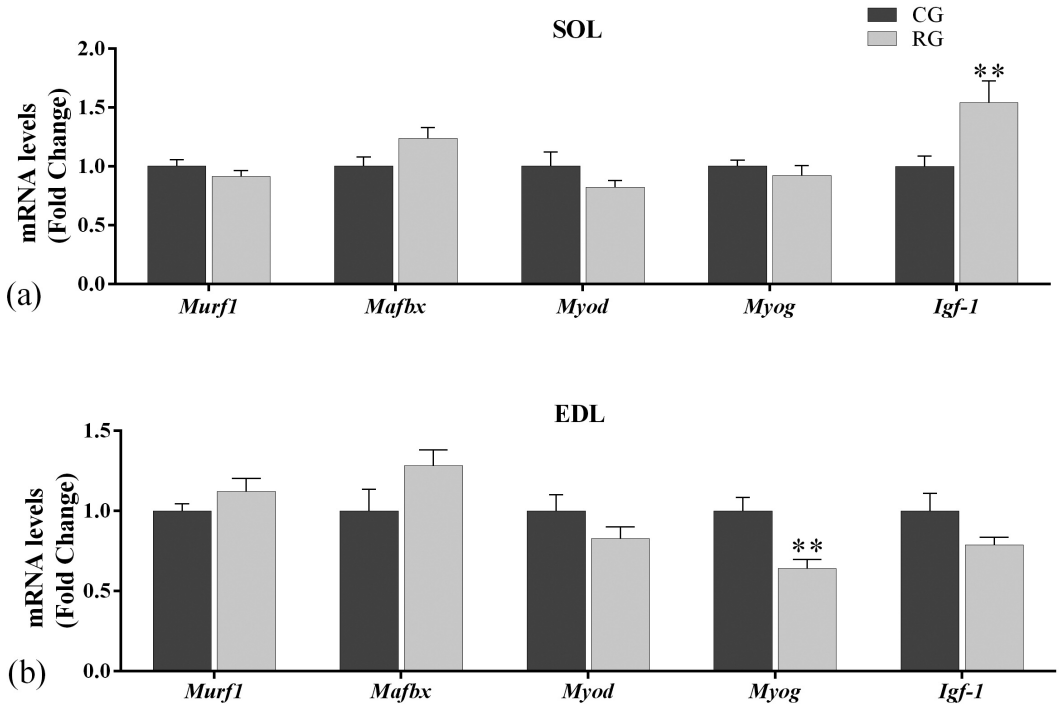

Fig. 6. Relative mRNA expression of anabolic, myogenic and catabolic genes in SOL and EDL muscles of the CG and RG groups. mRNA levels of the Murf1, Mafbx, Myod, Myog and Igf-1, of the SOL muscle **(a)**. Unpaired Mann Whitney test. mRNA levels of the Murf1, Mafbx, Myod, Myog and Igf-1, of the EDL muscle **(b)**. Unpaired Student's t-test. The data are expressed as fold change and are presented as the mean ± SEM (n=8). Unpaired Student's t-test. **p<0.01.

In the EDL muscle, only *Chad* gene (**p<0.01) increased the expression in the RG compared to the CG group (Fig. 8b).

Discussion

Our study analyzed the impacts of maternal protein restriction on the morphological and molecular characteristics of skeletal muscle fiber and extracellular matrix (ECM) components in aging offspring rats. Generally, we observed that the oxidative soleus (SOL) muscle is more prone to changed muscle fiber characteristics and gene expression associated with the ECM than to glycolytic and fast EDL muscle.

The decreased body weight in RG is an indication that protein restriction during the initial stages of development interposes the maintenance of body weight at aging. In fact, at birth, the protein restricted animals showed low body weight (data not shown). Using the same experimental conditions as used in our study, Santos et al. (2018) also showed a lower body weight of rats at birth and at aging, and Confortim et al. (2015), observed a lower body weight in adult rats. Considering these results, we can infer that protein restriction during the early life stages of rats strongly affects their body weight gain throughout life, as observed in our study.

Protein restriction of animals during pregnancy and lactation led to offspring with a decrease in the CSA in the SOL muscle, and in the gene expression of the oxidative marker *Sdha*, but no changes in muscle fiber

Table 7. List of the 101 differentially expressed genes (DEGs), upregulated or downregulated in the SOL muscle.

Symbol	Gene	Regulation
Aaed1	AhpC/TSA Antioxidant Enzyme Domain Containing 1	up
Abcb9	ATP Binding Cassette Subfamily B Member 9	down
Adam1a	ADAM Metallopeptidase Domain 1A	down
Adig	Adipogenin	up
Afap1l1	Actin Filament Associated Protein 1 Like 1	down
Ahnak2	AHNAK Nucleoprotein 2	down
Akap1	A-Kinase Anchoring Protein 1	down
Ankrd1	Ankyrin Repeat Domain 1	down
Apold1	Apolipoprotein L Domain Containing 1	down
Aqp7	Aquaporin 7	down
Arhgap24	Rho GTPase Activating Protein 24	down
Arntl	Aryl Hydrocarbon Receptor Nuclear Translocator Like	down
Ccdc28b	Coiled-Coil Domain Containing 28B	up
Ccdc92	Coiled-Coil Domain Containing 92	up
Chad	Chondroadherin	up
Clu	Clusterin	up
Clen3	Chloride Volatge-Gated Channel 3	down
Clenkb	Chloride Voltade-Gated Channel Kb	down
Cnp	2',3'-Cyclic Nucleotide 3' Phosphodiesterase	down
Cntn2	Contactin 2	up
Cpd	Carboxypeptidase D	up
Crhr2	Corticotropin Releasing Hormone Receptor 2	down
Cyp4f6	Cytochrome P450 Family 4 Subfamily F Member 3	down
Dgatl	Diacylglycerol O-Acyltransferase 1	up
Dgke	Diacylglycerol Kinase Epsilon	up
Dnaaf2	Dynein Axonemal Assembly Factor 2	down
Ephx1	Epoxide Hydrolase 1	up
Erp29	Endoplasmic Reticulum Protein 29	down
Fam213b	Family With Sequence Similarity 213 Member B	down
Fbox40	F-Box Protein 40	up
Fitm2	Fat Storage Inducing Transmembrane Protein 2	down
Fmod	Fibromodulin	up
Foxo1	Forkhead Box O1	down
Gstm7	Glutathione S- Transferase Mu	up
Hccs	Holocytochrome C Synthase	down
Hlf	HLF, PAR BZIP Transcription Factor	down
Hspb7	Heat Shock Protein Family B (Small) Member 7	down
Hspa5	Heat Shock Protein Family A (Hsp70) Member 5	up
Ids	Iduronate 2-Sulfatase	down
Ier3	Immediate Early Response 3	up
Ifrd1	Interferon Related Developmental Regulator 1	down
Kcnc.4	Potassium Voltage-Gated Channel Subfamily C Member 4	up
Klf10	Kruppel Like Factor 10	down
Klhl33	Kelch Like Family Member 33	up
Lrrc30	Leucine Rich Repeat Containing 30	up
Lsmem1	Leucine Rich Single-Pass Membrane Protein 1	up
Lsm10	LSM10, U7 Small Nuclear RNA Associated	up
Mcm4	Minichromosome Maintenance Complex Component 4	up
Mettl7	Methyltransferase Like 7A	up
Mfap4	Microfibril Associated Protein 4	up
Mlf1	Myeloid Leukemia Factor	up
Mmgt2	Membrane Magnesium Transporter2	down
Mpz	Myelin Protein Zero	down
Mtfp1	Mitochondrial Fission Process 1	down
c-Myc	MYC Proto-Oncogene, BHLH Transcription Factor	up
Mypop	Myb Related Transcription Factor, Partner Of Profilin	up
Naglt1	Major Facilitator Superfamily Domain Containing 4B	down
Neu3	Neuraminidase 3	down
Noct	Nocturnin	down
Nrep	Neuronal Regeneration Related Protein	up
Nuak1	NUAK Family Kinase 1	down
Ocrl	OCRL, Inositol Polyphosphate-5-Phosphatase	down
Odc1	Ornithine Decarboxylase	down
Pacrg	Parkin Coregulated	up
Pankl	Pantothenate Kinase 1	down
Phyhdl	Phytanoyl-CoA Dioxygenase Domain Containin	down
Plala	Phospholipase A1 Member A	down
Plin4	Perilipin 4	up
Pmepal	Prostate Transmembrane Protein, Androgen Induced 1	down
Pogk	Pogo Transposable Element Derived With KRAB Domain	down
Ppip5kl	Diphosphoinositol Pentakisphosphate Kinase 1	up
Pstpip2	Proline-Serine-Threonine Phosphatase Interacting Protein 2	down
Rapsn	Receptor Associated Protein Of The Synapse	up
Rhbdd1	Rhomboid Domain Containing 1	up
Rnf225	Ring Finger Protein 225	down
Sh3rf2	SH3 Domain Containing Ring Finger 2	down
Slc4la3	Solute Carrier Family 41 Member 3	down
Sikl	Salt Inducible Kinase 1	up
Slc25a22	Solute Carrier Family 25 Member 22	up
Tnnt3	Troponin T3	down
Tpml	Tropomyosin 1	down
Trafdl	TRAF-Type Zinc Finger Domain Containing 1	down
Tbxl5	T-Box 15	up
Tpd52	Tumor Protein D52	down
Trim 31	Tripartite Motif Containing 31	down
Uckll	Uridine-Cytidine Kinase 1 Like 1	up
Uspl6	Ubiquitin Specific Peptidase 16	up
Xpnpep3	X-Prolyl Aminopeptidase 3	down
YbeY	YbeY Metalloendoribonuclease	up
Zfp770	Zinc Finger Protein 770	down

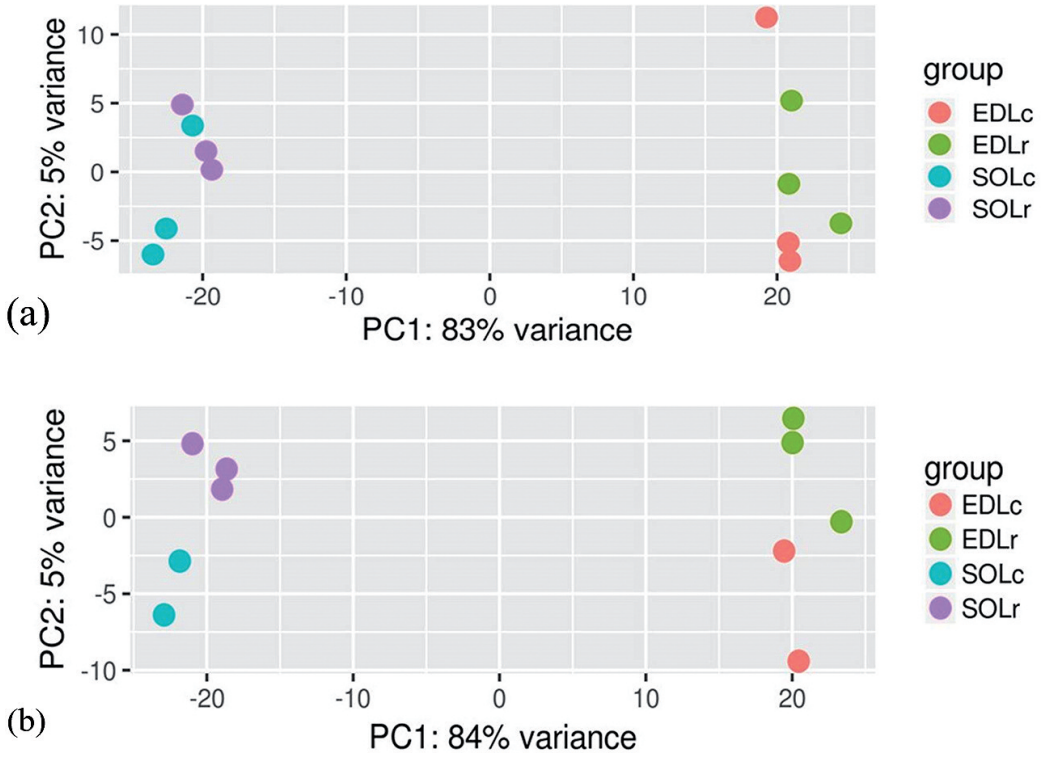

Fig. 7. Principal Component Analysis (PCA) showing the clustering of the SOL and EDL muscle samples. Samples sequenced from CG animals (blue, SOL muscle; red, EDL muscle), and RG animals (lilac, SOL muscle; green, EDL muscle) (n=3) **(a)**. Samples considered for bioinformatics analyses after one sample removed from both muscles; CG samples (blue, SOL muscle; red, EDL muscle), and RG samples (lilac, SOL muscle; green, EDL muscle) **(b)**.

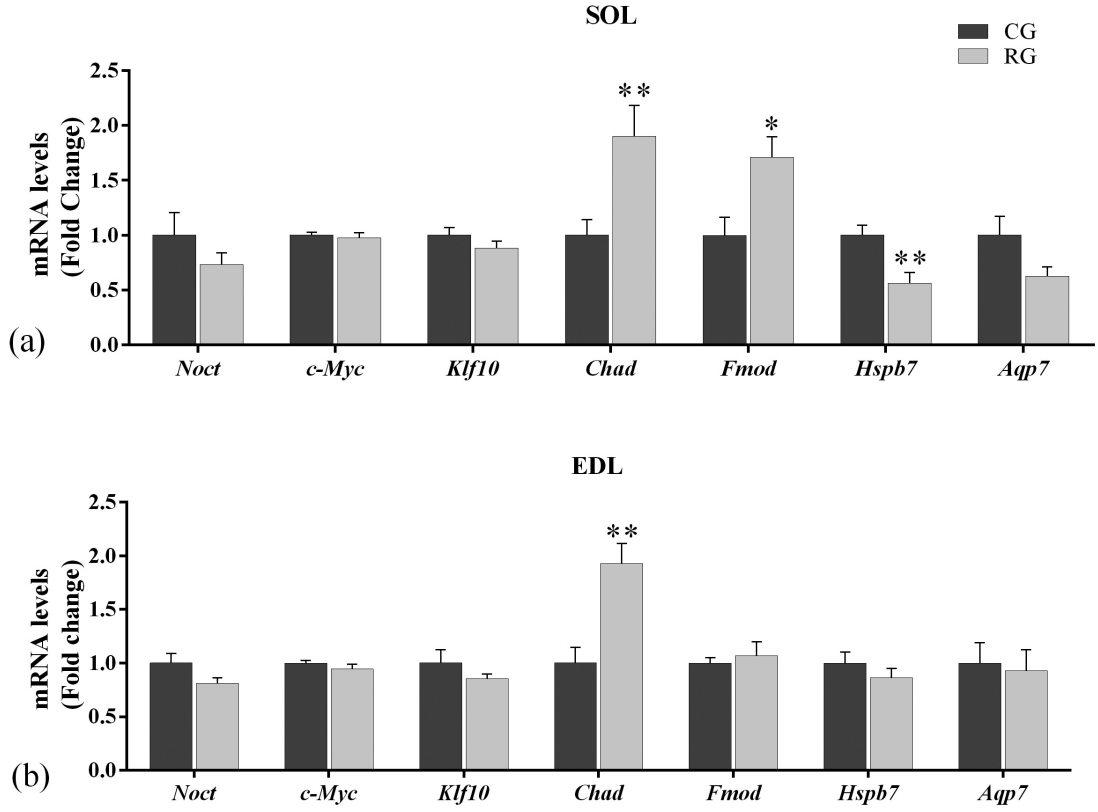

Fig. 8. Relative mRNA expression of genes involved with biogenesis, metabolism, and structural function pathways in SOL and EDL muscles of the CG and RG groups. mRNA levels of the Noct, c-Myc, Klf10, Chad, Fmod, Hspb7 and Aqp7, of the SOL muscle **(a)** mRNA levels of the Noct, c-Myc, Klf10, Chad, Fmod, Hspb7 and Aqp7, of the EDL muscle **(b)**. Data are expressed as fold change and are presented as the mean ± SEM (n=8). Unpaired Mann Whitney test. *p<0.05, **p<0.01.

types frequency. On the other hand, offspring EDL muscle presented with no changes in CSA or in *Sdha* gene expression, but an increase in glycolytic muscle fiber frequency. This result may be related to the difference in the metabolic and functional features of these muscles (Schiaffino and Reggiani, 2011; Schiaffino et al., 2013) which can determine the muscle-specific fiber type affected (Mallinson et al., 2007; Toscano et al., 2008; Cabeço et al., 2012). However, previous work has already shown that the SOL, a slow oxidative muscle, is more responsive to changes in offspring rats born to protein restricted mothers (Mallinson et al., 2007; Toscano et al., 2008; Cabeço et al., 2012; Confortin et al., 2015). Rehfeldt et al. (2012) explained that maternal protein restriction impairs myogenesis and muscle differentiation, culminating in a deficit in the myofiber number in piglets. These results strongly demonstrate that maternal protein restriction can restrict muscle growth potential in offspring, influencing muscle fiber number and muscle fiber CSA throughout life. This fact may explain the decreased CSA in the SOL muscle at aging observed in our study. Surprisingly, we did not find changes in atrogene mRNA expression indicating low catabolic activity in this condition and the decreased *Sdha* gene expression indicates a possible change in oxidative metabolism in the SOL at aging, although we did not observe any changes in muscle fiber frequency.

In the EDL muscle, a fast glycolytic muscle, we detected increased glycolytic metabolism and decreased *Myog* gene expression; however, no changes in CSA or in the *Sdha* gene expression were observed. Our results are in line with those of Cabeço et al. (2015) who showed increased glycolytic metabolism in the EDL muscle, in 112 day old rats, subjected to maternal protein restriction during pregnancy. In addition to myogenesis regulation, the MRFs *Myog* and *Myod* are also involved in muscle phenotype maintenance, controlling the slow/oxidative and fast/glycolytic phenotypes, respectively (Hughes et al., 1993; Seward et al., 2001; Alapat et al., 2009). Although a tendency to drive muscle metabolism from an oxidative pattern to glycolytic is commonly observed during aging (Caccia et al., 1979; Holloszy et al., 1991; Larsson et al., 1993), in our experiments, only the EDL muscle from the RG animals presented with decreased Myog expression. This result may indicate a protective mechanism of the glycolytic phenotype, a supposition corroborated by the unchanged *Sdha* and *CS* levels with the increased percentage of type IIB fiber frequency. The metabolic maintenance observed in the EDL muscle supports our

Table 8. List of the 53 differentially expressed genes (DEGs), upregulated or downregulated in the EDL muscle.

Symbol	Gene	Regulation
Acot2	Acyl-CoA Thioesterase 2	down
Acvr2b	Activin A Receptor Type 2B	up
Afalp1l1	Actin Filament Associated Protein 1 Like 1	up
Angptl2	Angiopoietin Like 2	up
Ankrd1	Ankyrin Repeat Domain 1	down
Apold1	Apolipoprotein L Domain Containing 1	down
Aqp7	Aquaporin 7	down
Arc	ActivityRegulated Cytoskeleton Associated Protein	down
Bcl6b	B Cell CLL/Lymphoma 6B	down
Btg2	BTG Anti-Proliferation Factor 2	down
Cc2d2a	Coiled-Coil And C2 Domain Containing 2A	up
Chad	Chondroadherin	up
Col24a1	Collagen Type XXIV Alpha 1 Chain	up
Clnd5	Claudin 5	down
Fam110d	Family With Sequence Similarity 110 Member D	up
Fam78a	Family With Sequence Similarity 78 Member A	up
Fam43a	Family With Sequence Similarity 43 Member A	down
Fmod	Fibromodulin	up
Hes1	Hes Family BHLH Transcription Factor 1	down
Hspb7	HeatShock Protein Family B (Small) Member 7	down
Id1	Inhibitor of DNA Binding 1, HLH Protein	down
Klf10	Kruppel Like Factor 10	down
Mlf1	Myeloid Leukemia Factor 1	up
Mlxip	MLX Interacting Protein	up
Mybph	Myosin Binding Protein H	down
c-Myc	MYC Proto-Oncogene, BHLH Transcription Factor	down
Noct	Nocturnin	down
Pml	Promyelocytic Leukemia	up
RGD1307461	Similar ao RIKEN cDNA 6430571L13; Similar a Proteína G20	up
Slco5a1	Solute Carrier Organic Anion Transporter Family Member 5A1	up
Tbc1d4	TBC1 Domain Family Member 4	up
Tead1	TEA Domain Transcription Factor 1	up
Thbs4	Thrombospondin 4	up
Tnik	TRAF2 and NCK Interacting Kinase	up
Wipf3	WAS/WASL Interacting Protein Family Member 3	up

Table 9. Differentially expressed genes (DEGs) involved with biogenesis, metabolism, and structural function pathways, selected for RT-qPCR validation.

Pathways	Genes/Symbol	Function	Reference
Biogenesis	Nocturnina (*Noct*)	Involved with embryogenesis and energy metabolism in adults	Nishikawa et al., 2013
	Proto-Oncogene Transcription Factor Myc (*c-Myc*)	Involved with cell proliferation and embryogenesis	Davis et al., 1993
	Kruppel Like Factor 10 (*Klf10*)	Transcriptional regulator related to cell proliferation and support of the Extracellular Matrix (ECM)	Parakati and DiMario, 2013
Metabolism	Nocturnin (*Noct*)	Involved with embryogenesis and energy metabolism in adults	Nishikawa et al., 2013
	Aquaporin (*Aqp7*)	Involved with muscle energy metabolism	Wakayama et al., 2014
Structural	Chondroadherin (*Chad*)	Associated with collagen and integrin in cartilage	Hessle et al., 2013
	Heat Shock Protein; Family B (*Small*); Member 7 (*Hspb7*)	Related to the structural support of skeletal muscle	Mercer et al., 2018
	Fibromodulin (*Fmod*)	Related to the structural organization of the Extracellular Matrix (ECM)	Lee et al., 2018b

hypothesis that this muscle is affected to a lesser degree in aged rats born to a dam fed a low protein diet during gestation and lactation.

Interestingly, maternal protein restriction increased the expression of *Igf-1* in the SOL muscle of aged offspring rats. *Igf-1* is a component of the IGF system regulating muscle protein synthesis under anabolic conditions (Schiaffino et al., 2013; Ascenzi et al., 2019). Recently, studies have also demonstrated IGF system components related to a protective mechanism in skeletal muscle. Paula et al. (2017) found an increase in *Igf-1* expression in pacu fish (*Piaractus mesopotamicus*) during ten days of fasting as a condition for maintaining metabolic homeostasis in skeletal muscle. Similarly, Miyazaki et al. (2019) observed activation of *Mtor*, a component of the *Igf-1* pathway, after hibernation of the Japanese black bear (*Ursus thibetanus japonicus*) as a mechanism of protection against muscular atrophy during food deprivation. In the same line, Ascenzi et al. (2019) detected a neutralizing effect of these IGF isoforms on sarcopenia in transgenic senile mice overexpressing the IGF-1Ea and IGF-1Eb isoforms, guaranteeing *Igf-1* production during mouse senility. Thus, we believe that the high *Igf-1* gene expression in the SOL muscle, the muscle affected to the greatest extent in our study, may be associated with the protective action of *Igf-1*, which acts as an activated sensor to maintain SOL muscle physiology under the conditions evaluated.

Transcriptome analysis led to the identification of common genes that are differentially expressed in both SOL and EDL muscles. They are related to biogenesis (*Noct, c-Myc* and *Klf10*) (Davis et al., 1993; Nishikawa et al., 2013; Parakati and DiMario, 2013), lipid metabolism (*Apq7*) (Wakayama et al., 2014), the cytoskeleton (*Hspb7*) (Juo et al., 2016), and structural muscle (*Fmod* and *Chad*) (Svensson et al., 1999; Hessle et al., 2013). Although the RT-qPCR validated genes exhibited the same expression pattern as that demonstrated by RNA-Seq, only *Chad, Fmod,* and *Hspb7* were significantly different in the RT-qPCR assessment. Comparisons between the validation obtained by RT-qPCR and that predicted by RNA-Seq data are widely used, although the validation rate is not fully compatible (Teng et al., 2016; Everaert et al., 2017). It is possible that the parameters used to establish the differentially expressed genes in our study may have influenced the number of genes, contributing to the difference in the prediction and validation of these differentially expressed genes.

The ECM of skeletal muscle is an essential component of the muscle tissue environment, it contributes to the maintenance of structural integrity and nutrition, and provides mechanotransduction support (Theocharis et al., 2016; Mendias et al., 2017; Ahmad et al., 2018). *Fmod*, a small leucine-rich proteoglycan (SLRP) is an essential regulator of ECM assembly that plays a dynamic role during muscle regeneration and in myogenesis controlling myoblast proliferation and differentiation (Lee et al., 2016, 2018a, 2018b; Ahmad et al., 2018). Svensson et al. (1999) showed that mice with *Fmod* knocked out exhibited an ECM that provided poor mechanical support due to the formation of thinner and abnormal collagen fibers in the tendon. *Chad*, another member of the SLRP family that is overexpressed in cartilage and bones, binds to collagen and interacts with integrins in the cell membrane (Shen et al., 1998; Haglund et al., 2011; Paracuellos et al., 2017).

Using RNA-Seq, our study is the first to demonstrate that the expression levels of *Fmod* and *Chad* were increased in SOL and EDL muscles of 540 day old rats born to dams that received low protein nutrition during pregnancy and lactation. The RT-qPCR analysis also showed increased *Chad* gene expression in both muscles, and *Fmod* only in the SOL muscle. The overexpression of these SLRPs may demonstrate the interaction between muscle and adjacent ECM, the maintenance of its components being necessary for the control of the SOL and EDL muscle phenotypes under the study conditions. We did not observe an increase in picrosirius red staining (data not shown) or in the gene expression of collagen 1a1 and collagen 3 (data not shown). Although we did not carry out a protein expression analysis of the changed genes, which we consider to be a limitation of this study, our transcriptome data validated by RT-qPCR showed that some ECM components are changed in aging rat offspring born to protein-restricted mothers, mainly in the SOL muscle.

Hspb7, a small heat shock protein of the chaperone system, is related to the protection and stabilization of the cytoskeleton during stress and the proteostasis of sarcomeres and sarcolemma (Vos et al., 2009; Juo et al., 2016; Mercer et al., 2018). Wu et al. (2017) demonstrated that embryos from mice with *Hspb7* knocked out showed disorganized sarcomeres that impaired contractile muscle function. In addition, Juo et al. (2016) observed mice with *Hspb7* knocked out and found myofibrillar disorganization in the diaphragm muscle, demonstrating that the deficiency of this gene is associated with changes in sarcomere integrity and a decrease in respiratory capacity. In our experiment, *Hspb7* expression was downregulated in RNA-Seq analysis for both the SOL and EDL muscles in the RG animals, and RT-qPCR analysis revealed a decrease in gene expression only in the SOL muscle. Toscano et al. (2008) demonstrated that maternal protein restriction changed the biomechanical properties of the SOL and EDL muscles of young and adult rat offspring. Although functional tests have not been performed in the present study, it is possible that the muscle contractile function of aged animals born to protein-restricted dams was compromised, particularly the oxidative SOL muscle, as the aging condition, per se, is closely linked with decreased muscle strength (Janssen, 2006; Sakuma and Yamaguchi, 2012).

Because of the importance of the ECM in maintaining muscle integrity, we believe that the

overexpression of the *Fmod* and *Chad* genes, mainly in the SOL muscle, may indicate a possible reorganization of some ECM muscle components in aged rats previously exposed to a low protein diet during pregnancy and lactation. This ECM rearrangement may occur in order to minimize the effects of the process during aging. Further studies are needed to evaluate the protein expression of the changed ECM genes observed in our study, and an analysis of the structural and sarcomeric proteins of the muscle fibers is important to better understand the impact of maternal protein malnutrition on the muscle microenvironment of offspring.

Collectively, our molecular, immunohistochemical and morphological data showed that maternal protein restriction promoted changes in muscle morphology and in the expression of metabolic, myogenic, and structural genes, mainly in the oxidative SOL muscle, in their aged rat offspring.

Acknowledgements. We thank the Extracellular Matrix Laboratory group for their assistance during this work; the Electron Microscopy Center, Institute of Biosciences, Botucatu, UNESP, for the use of their Facilities Services; and Sarah Santiloni Cury for the help in the fractal analysis.
Competing interests. No competing interests declared.
Financial Support. This work was supported by the Coordination for the Improvement of Higher Education Personnel (CAPES) [Code 001/ Grant number 88887.338844/2019-00], to finance JSV, and by Sao Paulo Research Foundation (FAPESP), [Grants numbers 2017/11230-8 and 2019/01592-5] to finance ESP and MDP.
Data availability. Raw and processed data are available in the Gene Expression Omnibus database under accession number GSE137094.
Author Contributions. Conceptualization: JSV MDP LAJ BEAF RFC. Data Curation: JSV BEAF. Formal analysis: JSV ESP BPSD TGP. Funding acquisition: MDP LAJ RFC. Investigation: JSV ESP BTTZ MD. Methodology: JSV SAAS LAJ. Project administration: JSV MDP. Resources: MDP RFC LAJ. Software: BEAF RFC. Supervision: MDP LAJ BEAF. Validation: JSV ESP MDP SAAS LAJ. Visualization: JSV ESP. Writing ± original draft: JSV ESP MDP. Writing ± review & editing: JSV ESP MDP RFC.

References

Ahmad K., Lee E.J., Moon J.S., Park S.-Y. and Choi I. (2018). Multifaceted interweaving between extracellular matrix, insulin resistance, and skeletal muscle. Cells 7, 148-163.

Alapat D.V, Chaudhry T., Ardakany-Taghavi R. and Kohtz D.S. (2009). Fiber-types of sarcomeric proteins expressed in cultured myogenic cells are modulated by the dose of myogenin activity. Cell. Signal. 21, 128-135.

Anders S. and Huber W. (2010). Differential expression analysis for sequence count data. Genome Biol. 11, R106.

Ascenzi F., Barberi L., Dobrowolny G., Villa Nova Bacurau A., Nicoletti C., Rizzuto E., Rosenthal N., Scicchitano B. M. and Musarò A. (2019). Effects of IGF-1 isoforms on muscle growth and sarcopenia. Aging Cell 18, e12954.

Barker D.J.P. (1998). In utero programming of chronic disease. Clin. Sci. 95, 115-128.

Barker D.J.P. (2004). Developmental origins of adult health and disease. J. Epidemiol. Community Heal. 58, 114-115.

Bolger A.M., Lohse M. and Usadel B. (2014). Trimmomatic: a flexible trimmer for Illumina sequence data. Bioinformatics 30, 2114-2120.

Cabeço L.C., Budri P.E., Baroni M., Castan E.P., Carani F.R., de Souza P.A.T., Boer P.A., Matheus S.M.M. and Dal-Pai-Silva M. (2012). Maternal protein restriction induce skeletal muscle changes without altering the MRFs MyoD and myogenin expression in offspring. J. Mol. Histol. 43, 461-471.

Caccia M.R., Harris J.B. and Johnson M.A. (1979). Morphology and physiology of skeletal muscle in aging rodents. Muscle Nerve 2, 202-212.

Carlson M.E., Suetta C., Conboy M.J., Aagaard P., Mackey A., Kjaer M. and Conboy I. (2009). Molecular aging and rejuvenation of human muscle stem cells. EMBO Mol. Med. 1, 381-391.

Confortim H.D., Jerônimo L.C., Centenaro L.A., Felipe Pinheiro P.F., Brancalhão R.M.C., Matheus S.M.M. and Torrejais M.M. (2015). Effects of aging and maternal protein restriction on the muscle fibers morphology and neuromuscular junctions of rats after nutritional recovery. Micron 71, 7-13.

Confortim H.D., Jerônimo L.C., Centenaro L.A., Pinheiro P.F.F., Matheus S.M.M. and Torrejais M.M. (2017). Maternal protein restriction during pregnancy and lactation affects the development of muscle fibers and neuromuscular junctions in rats. Muscle Nerve 55, 109-115.

Davis A.C., Wims M., Spotts G.D., Hann S. R. and Bradley A. (1993). A null c-myc mutation causes lethality before 10.5 days of gestation in homozygotes and reduced fertility in heterozygous female mice. Genes Dev. 7, 671-682.

Domingues-Faria C., Vasson M.-P., Goncalves-Mendes N., Boirie Y. and Walrand S. (2016). Skeletal muscle regeneration and impact of aging and nutrition. Ageing Res. Rev. 26, 22-36.

Everaert C., Luypaert M., Maag J.L.V., Cheng Q.X., Marcel E., Hellemans J. and Mestdagh P. (2017). Benchmarking of RNA-sequencing analysis workflows using whole- transcriptome RT-qPCR expression data. Sci. Rep. 7, 1559-1570.

Fleige S. and Pfaffl M.W. (2006). RNA integrity and the effect on the real-time qRT-PCR performance. Mol. Aspects Med. 27, 126-139.

Haglund L., Tillgren V., Addis L., Wenglén C., Recklies A. and Heinegård D. (2011). Identification and characterization of the integrinα2β1 binding motif in chondroadherin mediating cell attachment. J. Biol. Chem. 286, 3925-3934.

Hales C.N. and Barker D.J.P. (2001). The thrifty phenotype hypothesis. Br. Med. Bull. 60, 5-20.

Hanson M. (2015). The birth and future health of DOHaD. J. Dev. Orig. Health Dis. 6, 434-437.

Hessle L., Stordalen G.A., Wenglén C., Petzold C., Tanner E.K., Brorson S.-H., Baekkevold E.S., Önnerfjord P., Reinholt F.P. and Heinegård D. (2013). The skeletal phenotype of chondroadherin deficient mice. PLoS One 8, e63080.

Holloszy J.O., Chen M., Cartee G.D. and Young J.C. (1991). Skeletal muscle atrophy in old rats: differential changes in the three fiber types. Mech. Ageing Dev. 60, 199-213.

Hughes S.M., Taylor J.M., Tapscott S.J., Gurley C.M., Carter W.J. and Peterson C.A. (1993). Selective accumulation of MyoD and myogenin mRNAs in fast and slow adult skeletal muscle is controlled by innervation and hormones. Development 118, 1137-1147.

Janssen I. (2006). Influence of sarcopenia on the development of physical disability: the cardiovascular health study. J. Am. Geriatr.

Soc. 54, 56-62.

Juo L.-Y., Liao W.-C., Shih Y.-L., Yang B.-Y., Liu A.-B. and Yan Y.-T. (2016). HSPB7 interacts with dimerized FLNC and its absence results in progressive myopathy in skeletal muscles. J. Cell Sci. 129, 1661-1670.

Kalbe C., Lösel D., Block J., Lefaucheur L., Brüssow K.-P., Bellmann O., Pfuhl R., Puppe B., Otten W., Metges C.C. and Rehfeldt C. (2017). Moderate high or low maternal protein diets change gene expression but not the phenotype of skeletal muscle from porcine fetuses. Domest. Anim. Endocrinol. 58, 63-75.

Kilkenny C., Browne W., Cuthill I.C., Emerson M. and Altman D.G. (2010). Animal research: reporting in vivo experiments: the ARRIVE guidelines. Br. J. Pharmacol. 160, 1577-1579.

Larsson L., Biral D., Campione M. and Schiaffino S. (1993). An age-related type IIB to IIX myosin heavy chain switching in rat skeletal muscle. Acta Physiol. Scand. 147, 227-234.

Leandro C.G., Ribeiro W.S., dos Santos J.A., Bento-Santos A., Lima-Coelho C.H., Falcão-Tebas F., Lagranha C.J., Lopes-de-Souza S., Manhães-de-Castro R. and Toscano A.E. (2012). Moderate physical training attenuates muscle-specific effects on fibre type composition in adult rats submitted to a perinatal maternal low-protein diet. Eur. J. Nutr. 51, 807-815.

Lee E.J., Jan A.T., Baig M.H., Ashraf J.M., Nahm S.-S., Kim Y.-W., Park S.-Y. and Choi I. (2016). Fibromodulin: a master regulator of myostatin controlling progression of satellite cells through a myogenic program. FASEB J. 30, 2708-2719.

Lee E.J., Jan A.T., Baig M.H., Ahmad K., Malik A., Rabbani G., Kim T., Lee I.K., Lee Y.H., Park S.Y. and Choi I. (2018a). Fibromodulin and regulation of the intricate balance between myoblast differentiation to myocytes or adipocyte-like cells. FASEB J. 32, 768-781.

Lee E.J., Nam J.H. and Choi I. (2018b). Fibromodulin modulates myoblast differentiation by controlling calcium channel. Biochem. Biophys. Res. Commun. 503, 580-585.

Li B. and Dewey C. N. (2011). RSEM: accurate transcript quantification from RNA-Seq data with or without a reference genome. BMC Bioinformatics 12, 323-336.

Liao Y., Smyth G.K. and Shi W. (2014). FeatureCounts: an efficient general purpose program for assigning sequence reads to genomic features. Bioinformatics 30, 923-930.

Livak K.J. and Schmittgen T.D. (2001). Analysis of relative gene expression data using real-time quantitative PCR and the 2(-Delta Delta C(T)) methods. Methods 25, 402-408.

Mallinson J.E., Sculley D.V, Craigon J., Plant R., Langley-Evans S.C. and Brameld J.M. (2007). Fetal exposure to a maternal low-protein diet during mid-gestation results in muscle-specific effects on fibre type composition in young rats. Br. J. Nutr. 98, 292-299.

Mendias C.L., Schwartz A.J., Grekin J.A., Gumucio J.P. and Sugg K.B. (2017). Changes in muscle fiber contractility and extracellular matrix production during skeletal muscle hypertrophy. J. Appl. Physiol. 122, 571-579.

Mercer E.J., Lin Y.-F., Cohen-Gould L. and Evans T. (2018). Hspb7 is a cardioprotective chaperone facilitating sarcomeric proteostasis. Dev. Biol. 435, 41-55.

Miyazaki M., Shimozuru M. and Tsubota T. (2019). Skeletal muscles of hibernating black bears show minimal atrophy and phenotype shifting despite prolonged physical inactivity and starvation. PLoS One 14, e0215489.

Nishikawa S., Hatanaka Y., Tokoro M., Shin S.-W., Shimizu N., Nishihara T., Kato R., Takemoto A., Amano T., Anzai M., Hosoi S., Matsumoto K. (2013). Functional analysis of nocturnin, a circadian deadenylase, at maternal-to-zygotic transition in mice. J. Reprod. Dev. 59, 258-265.

Paracuellos P., Kalamajski S., Bonna A., Bihan D., Farndale R.W. and Hohenester E. (2017). Structural and functional analysis of two small leucine-rich repeat proteoglycans, fibromodulin and chondroadherin. Matrix Biol. 63, 106-116.

Parakati R. and DiMario J.X. (2013). Repression of myoblast proliferation and fibroblast growth factor receptor 1 promoter activity by Klf10 protein. J. Biol. Chem. 288, 13876-13884.

Paula T.G., Zanella B.T.T., Fantinatti B.E.A., Moraes L.N., Duran B.O. S., Oliveira C.B., Salomão R.A.S., Silva R.N., Padovani C.R., Santos V.B., Mareco E.A., Carvalho R.F and Dal-Pai-Silva M. (2017). Food restriction increase the expression of mTORC1 complex genes in the skeletal muscle of juvenile pacu (Piaractus mesopotamicus). PLoS One 12, e0177679.

Raja J.S., Hoffman M.L., Govoni K.E., Zinn S.A. and Reed S.A. (2016). Restricted maternal nutrition alters myogenic regulatory factor expression in satellite cells of ovine offspring. Animal 10, 1200-1203.

Reeves P.G., Nielsen F.H. and Fahey G.C. (1993). AIN-93 purified diets for laboratory rodents: final report of the american institute of nutrition ad hoc writing committee on the reformulation of the ain-76a rodent diet. J. Nutr. 123, 1939-1951.

Rehfeldt C., Lefaucheur L., Block J., Stabenow B., Pfuhl R., Otten W., Metges C.C. and Kalbe C. (2012). Limited and excess protein intake of pregnant gilts differently affects body composition and cellularity of skeletal muscle and subcutaneous adipose tissue of newborn and weanling piglets. Eur. J. Nutr. 51, 151-165.

Sakuma K. and Yamaguchi A. (2012). Sarcopenia and cachexia: the adaptations of negative regulators of skeletal muscle mass. J. Cachexia. Sarcopenia Muscle 3, 77-94.

Santos S.A.A., Camargo A.C., Constantino F.B., Colombelli K.T., Mani F., Rinaldi J.C., Franco S., Portela L.M.F., Duran B.O.S., Scarano W.R., Hinton B.T., Felisbino S.L. and Justulin L.A. (2018). Maternal low-protein diet impairs prostate growth in young rat offspring and induces prostate carcinogenesis with aging. J. Gerontol. A Biol. Sci. Med. Sci. 74, 751-759.

Schiaffino S. and Reggiani C. (2011). Fiber types in mammalian skeletal muscles. Physiol. Rev. 91, 1447-1531.

Schiaffino S., Dyar K.A., Ciciliot S., Blaauw B. and Sandri M. (2013). Mechanisms regulating skeletal muscle growth and atrophy. FEBS J. 280, 4294-4314.

Schneider C.A., Rasband W.S. and Eliceiri K.W. (2012). NIH image to ImageJ: 25 years of image analysis. Nat. Methods 9, 671-675.

Seward D.J., Haney J.C., Rudnicki M.A. and Swoap S.J. (2001). bHLH transcription factor MyoD affects myosin heavy chain expression pattern in a muscle-specific fashion. Am. J. Physiol. Physiol. 280, C408-C413.

Shen Z., Gantcheva S., Månsson B., Heinegård D. and Sommarin Y. (1998). Chondroadherin expression changes in skeletal development. Biochem. J. 330, 549-557.

Stearns-Reider K.M., D'Amore A., Beezhold K., Rothrauff B., Cavalli L., Wagner W.R., Vorp D.A., Tsamis A., Shinde S., Zhang C., Barchowsky A., Rando T.A., Tuan R.S. and Ambrosio F. (2017). Aging of the skeletal muscle extracellular matrix drives a stem cell fibrogenic conversion. Aging Cell 16, 518-528.

Svensson L., Aszódi A., Reinholt F.P., Fässler R., Heinegård D. and Oldberg Å. (1999). Fibromodulin-null mice have abnormal collagen fibrils, tissue organization, and altered lumican deposition in tendon.

J. Biol. Chem. 274, 9636-9647.

Talbert E.E. and Guttridge D.C. (2016). Impaired regeneration: A role for the muscle microenvironment in cancer cachexia. Semin. Cell Dev. Biol. 54, 82-91.

Teng M., Love M.I., Davis C.A., Djebali S., Dobin A., Graveley B.R., Li S., Mason C.E., Olson S., Pervouchine D., Sloan C.A., Wei X., Zhan L. and Irizarry R.A. (2016). A benchmark for RNA-seq quantification pipelines. Genome Biol. 17, 74. Erratum in Genome Biol. 17, 203 (2016).

Theocharis A.D., Skandalis S.S., Gialeli C. and Karamanos N.K. (2016). Extracellular matrix structure. Adv. Drug Deliv. Rev. 97, 4-27.

Toscano A.E., Manhães-de-Castro R. and Canon F. (2008). Effect of a low-protein diet during pregnancy on skeletal muscle mechanical properties of offspring rats. Nutrition 24, 270-278.

Vechetti-Júnior I.J., Aguiar A.F., De Souza R.W.A., Almeida F.L.A., De Almeida Dias H.B., De Aguiar Silva M. A., Carani F.R., Ferraresso R.L.P., Carvalho R.F. and Dal-Pai-Silva M. (2013). NFAT isoforms regulate muscle fiber type transition without altering can during aerobic training. Int. J. Sports Med. 34, 861-867.

Vechetti I.J., Bertaglia R.S., Fernandez G.J., De Paula T.G., De Souza R.W.A., Moraes L.N., Mareco E.A., De Freitas C.E.A., Aguiar A.F., Carvalho R.F., and Dal-Pai-Silva M (2016). Aerobic exercise recovers disuse-induced atrophy through the stimulus of the LRP130/PGC-1α complex in aged rats. J. Gerontol. A Biol. Sci. Med. Sci. 71, 601-609.

Velleman S.G. (1999). The role of the extracellular matrix in skeletal muscle development. Poult. Sci. 78, 778-784.

Vos M.J., Kanon B. and Kampinga H.H. (2009). HSPB7 is a SC35 speckle resident small heat shock protein. Biochim. Biophys. Acta 1793, 1343-1353.

Voytik S.L., Przyborski M., Badylak S.F. and Konieczny S.F. (1993). Differential expression of muscle regulatory factor genes in normal and denervated adult rat hindlimb muscles. Dev. Dyn. 198, 214-224.

Wakayama Y., Hirako S., Ogawa T., Jimi T. and Shioda S. (2014). Upregulated expression of Aqp7 in the skeletal muscles of obese OB/OB mice. Acta Histochem. Cytochem. 47, 27-33.

Wen Y., Murach K.A., Vechetti I.J., Fry C.S., Vickery C., Peterson C.A., McCarthy J.J. and Kenneth S Campbell K.S. (2018). MyoVision: software for automated high-content analysis of skeletal muscle immunohistochemistry. J. Appl. Physiol. 124, 40-51.

Wu T., Mu Y., Bogomolovas J., Fang X., Veevers J., Nowak R.B., Pappas C.T., Gregorio C.C., Evans S.M., Fowler V.M. and Chen J. (2017). HSPB7 is indispensable for heart development by modulating actin filament assembly. Proc. Natl. Acad. Sci. USA 114, 11956-11961.

Yang I.S. and Kim S. (2015). Analysis of whole transcriptome sequencing data: workflow and software. Genomics Inform. 13, 119-125.

Accepted April 12, 2021